Kovove Mater. 50 2012 399–406
DOI: 10.4149/km_2012_6_399

Characterization of the Al-13Si-10Fe alloy produced by centrifugal atomization and ultra-high-pressure compaction

F. Průša[1]*, D. Vojtěch[1], K. Dám[1,2]

[1] *Department of Metals and Corrosion Engineering, Institute of Chemical Technology, Prague, Technická 5, 166 28 Prague 6, Czech Republic*
[2] *Institute of Physics of the Academy of Sciences of the Czech Republic, Na Slovance 2, 182 21 Prague 8, Czech Republic*

Received 31 January 2012, received in revised form 29 August 2012, accepted 3 September 2012

Abstract

An Al-13Si-10Fe (wt.%) alloy was prepared via melt centrifugal atomization and compaction at a pressure of 6 GPa. The compact was porosity-free with good contacts between particles. The structure was very fine and consisted of primary α(Al) dendrites, eutectic silicon and needles of the β-Al_5FeSi phase. The Vickers hardness and compressive strength were 185 HV and 720 MPa, respectively. Surprisingly, the as-compacted alloy exhibited a certain degree of plasticity due to the refined morphology of needles. The alloy was annealed at 300–500 °C for 100 h, and both the growth of Si particles and fragmentation of β-Al_5FeSi particles were observed. Structural transformations resulted in both a slow reduction of hardness and strength and a significant increase of plasticity. When the thermal stability of the Al-13Si-10Fe alloy was compared to that of the casting Al-12Si-1Cu-1Mg-1Ni alloy commonly utilized in the automotive industry for pistons for combustion engines, it was found to be superior.

K e y w o r d s: aluminium, Al-Si-Fe alloy, rapid solidification, structure, mechanical properties

1. Introduction

Al-Si based alloys show a high strength-to-weight ratio, high thermal conductivity and excellent castability. These characteristics make them of interest for the fabrication of various light-weight components in the automotive and aerospace industries (for engine blocks, cylinder heads, pistons, etc.). Millions of these components are produced every year by gravity or die casting. The addition of elements that are slow diffusers in Al to these alloys improves their thermal stability, which is important for the fabrication of thermally loaded parts, such as pistons and turbocharger rotors. Figure 1 shows that transition metals (TMs) like Fe or Cr are very effective to this end [1]. However, the concentrations of transition metals in casting and wrought Al alloys are strongly limited. At most, only a few weight percents of TMs may be utilized in these alloys because higher concentrations would produce excessive fractions of hard and brittle intermetallic phases in the structure deteriorating mechanical properties.

Powder metallurgy (PM) is a route which enables the preparation of qualitatively new Al-based alloys containing TMs in concentrations far exceeding those in common casting and wrought alloys [2]. Rapid solidification of a melt, which generally occurs in powder preparation, refines the structure, reduces the volume fraction of intermetallic phases and forms new metastable crystalline, quasi-crystalline and amorphous phases [2]. All of these structural features are beneficial for achieving desirable combinations of strength, ductility and thermal stability. Powder compaction is generally performed by pressing and sintering or by hot extrusion [3]. Through the proper adjustment of compaction parameters (temperature, time, rate), the beneficial structural parameters can be retained in the bulk alloy.

Recently, rapidly solidified, PM Al-Si-Fe based alloys containing up to 5 wt.% Fe were studied and shown to have a good combination of strength and

*Corresponding author: tel.: +420 220444550; fax: +420 220444400; e-mail address: Filip.Prusa@vscht.cz

Table 1. Chemical composition (wt.%) of the investigated alloys

Material (preparation)	Element (wt.%)										
	Mg	Si	Ca	Ti	Cr	Mn	Fe	Ni	Cu	Zn	Al
Al-13Si-10Fe (PM)	0.25	13.03	0.11	0.04	0.05	0.13	9.64	0.03	0.04	0.11	bal.
Al-12Si-1Cu-1Mg-1Ni (casting, T6 heat treatment)	1.02	11.83	0.05	0.12	0.05	0.19	0.15	0.90	1.18	0.03	bal.

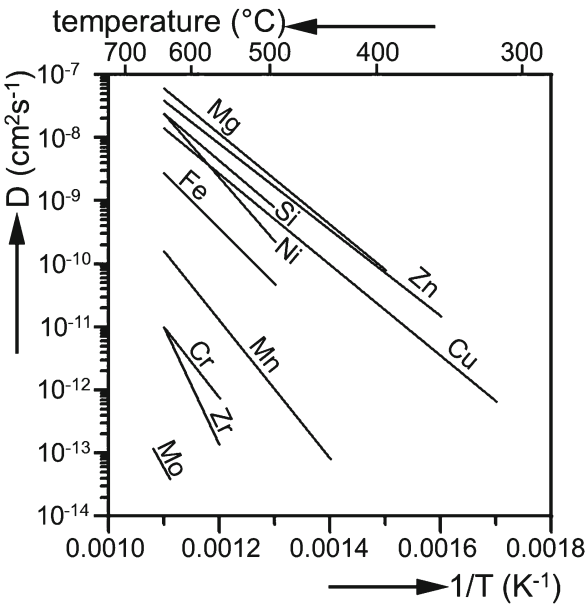

Fig. 1. Arrhenius plots of diffusion coefficients, D, of various metals in Al [1]. Transition metals like Fe, Cr or Ti have significantly lower diffusion coefficients when compared with the commonly used alloying elements like Cu, Si or Mg.

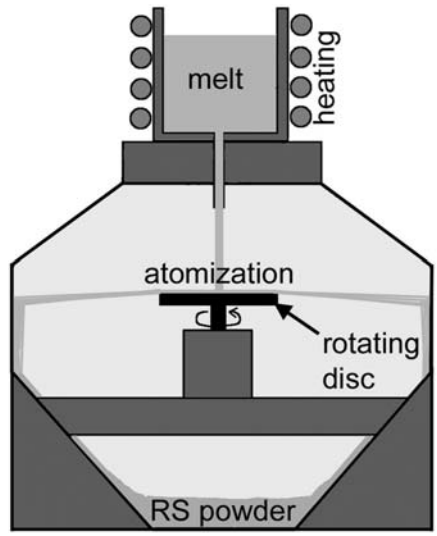

Fig. 2. Schematic drawing of centrifugal atomization producing rapidly solidified (RS) powders.

thermal stability [4–7]. The Al-Si-Fe alloys are promising for future structural applications, specifically because they are inexpensive. Moreover, the scraps used in Al recycling commonly contain high fractions of Fe, which currently must be removed. Thus, PM offers a way to directly process Fe-containing wastes.

In this study, we investigate a PM alloy containing a significantly higher concentration (10 wt.%) of thermally stabilizing Fe. The alloy is compacted by pressing at an ultra-high-pressure of 6 GPa. This method was recently shown to provide sufficiently compact and porosity-free Al-based materials [8]. We demonstrate that such a highly alloyed material, when processed by PM, exhibits not only high strength and thermal stability but also acceptable ductility. In addition, remarkable structural refining, which occurs during thermal exposition of this alloy, is demonstrated.

2. Experimental

A PM alloy with a nominal chemical composition of Al-13Si-10Fe is studied in this work. The PM alloy is compared with a commercial Al-Si-based casting alloy with a nominal composition of Al-12Si-1Cu-1Mg-1Ni. This alloy is generally considered as highly thermally stable, and therefore it is widely used in the automotive industry for the production of thermally loaded components, such as pistons. The chemical composition of both investigated materials is given in Table 1.

The Al-13Si-10Fe alloy was prepared by melting pure elements and master alloys in a vacuum induction furnace under an argon atmosphere. After a sufficient homogenization of the melt was achieved, the melt was poured into a cast iron metal mould to prepare an ingot 20 mm in diameter and 150 mm in length. Rapidly solidified powder was prepared by centrifugal atomization, which is schematically shown in Fig. 2. The alloy ingot was re-melted under argon and ejected onto a rapidly rotating graphite wheel (rotation speed of 30 000 rpm) to produce flake-like particles (Fig. 3). The dimensions of the powder particles ranged from 0.1 to 2 mm with a thickness of approximately 50 μm. Afterwards, the rapidly solidified powder was placed

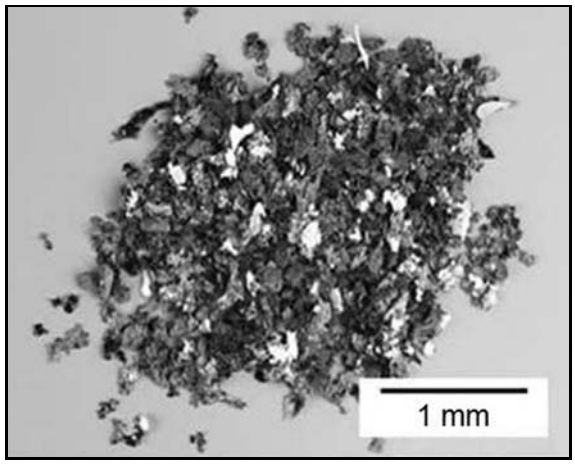

Fig. 3. Flake-like powder particles prepared by centrifugal atomization.

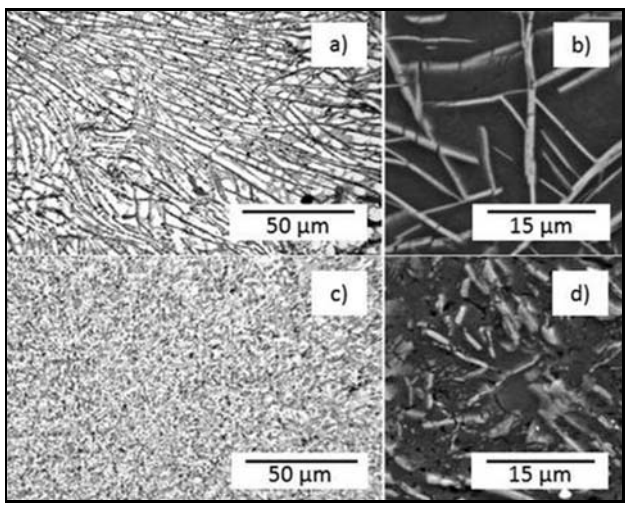

Fig. 4. Optical and detailed SEM micrographs of the Al-13Si-10Fe alloy: a), b) as-compacted; c), d) annealed at 500 ℃/100 h (silicon particles are hardly distinguished in SEM micrographs due to a weak secondary electron contrast).

into a tungsten carbide mould and was compacted by uni-axial pressing at an ultra-high pressure of 6 GPa to prepare cylindrical samples 15 mm in diameter and 5 mm in height. The pressing temperature and time were limited to 300 ℃ and 5 min, respectively, to prevent excessive structural coarsening. It should be noted that the pressure applied in our experiment was one order of magnitude greater than the pressures commonly used for uni-axial or isostatic pressing of powders. In the following text, the alloy prepared by the procedure above will be denoted as "as-compacted".

The casting alloy was provided by an industrial supplier in the form of an ingot with a thickness of 30 mm and a length of 150 mm. The alloy was heat treated by the T6 regime consisting of solution annealing at 510 ℃/5 h, water quenching and artificial ageing at 230 ℃/6 h [9].

For both of the investigated materials, compressive mechanical properties were measured with an Instron 5882 machine at a deformation rate of 1 mm min^{-1}. Vickers hardness tests were performed at room temperature with a 5 kg load. To examine the thermal stability of the alloys, compressive tests were also performed after annealing the samples for 100 h at 300–500 ℃, and the room temperature Vickers hardness' development was observed to follow structural changes induced by the long annealing time.

The structures of the alloys were investigated using light microscopy (LM), scanning electron microscopy (SEM, Tescan Vega 3) and energy dispersion spectrometry (EDS, Oxford Instruments Inca 350). The phase composition was determined by X-ray diffraction (XRD, X Pert Pro).

3. Results and discussion

3.1. Structure

The structure of the Al-13Si-10Fe alloy is shown in Fig. 4. The as-compacted alloy (Fig. 4a) contains three structural components: primary α(Al) dendrites, α(Al) + Si interdendritic eutectic and needle-like intermetallic phases. The primary dendrites are very fine, and the average distance between dendritic branches is 5 µm. Also, eutectic silicon particles appear to be refined, and their size does not exceed 1 µm. The needle-like particles have an average thickness of 2 µm and length of 30 µm.

The observed structural refining is a direct consequence of rapid solidification occurring during the centrifugal atomization of the melt. In this process (Fig. 2), the melt stream falls onto a fast rotating wheel where it is broken into small droplets by the centrifugal force. These droplets are ejected towards the cooled wall of the atomizer where they rapidly solidify and obtain the typical flake-like shape. It will be shown later that the structural refining has a positive impact on the resulting mechanical properties. Although the centrifugal atomization does not provide as high cooling rates as, for example, melt spinning or gas atomization, these cooling rates are still much higher than those achieved in the classical gravity casting processes ($\sim$ 5 K s^{-1}). Moreover, the centrifugal atomization is able to produce large quantities of rapidly solidified powders at low cost.

It is also important to notice in Fig. 4a that the as-compacted alloy shows almost no porosity and very good contacts between particles. Apparently, sufficient diffusion bonding between the particles was induced by ultra-high pressure of 6 GPa used in this experi-

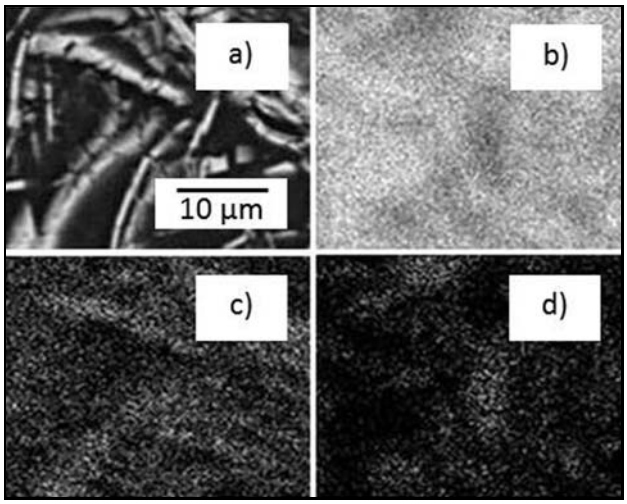

Fig. 5. Element distribution maps of the as-compacted Al-13Si-10Fe alloy (SEM, EDS): a) image, b) Al, c) Si, d) Fe.

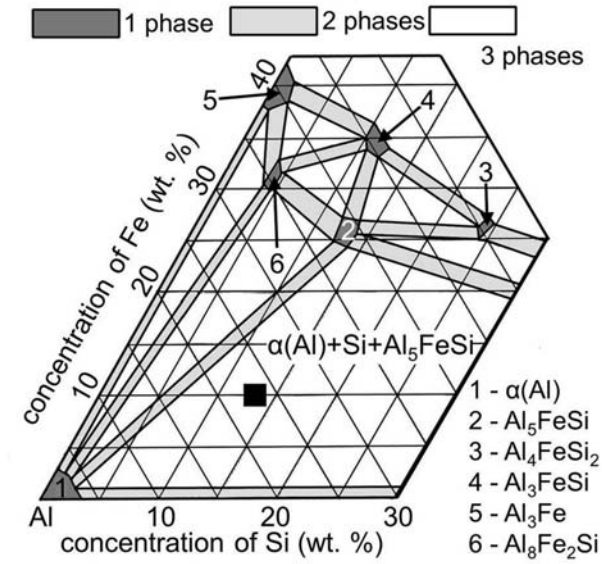

Fig. 7. Aluminium corner of the Al-Si-Fe phase diagram [10] (the chemical composition of the investigated alloy is marked by a black cube).

ment. A similar finding, where an almost porosity-free and compact material had formed, was also reported by Cieslak et al. [8]. Ultra-high-pressure compression at relatively low temperatures and short times can therefore be considered as an alternative to classical hot extrusion which is generally performed at 400 ℃ and more. The advantage of this alternative is the minimization of structural coarsening at high temperatures.

Figure 5 illustrates the element distribution in the as-compacted Al-13Si-10Fe alloy. Eutectic silicon particles are barely seen in this map because of their small dimensions. It is observed that the needle-like particles are enriched by both Fe and Si, so that they correspond to the ternary β-Al_5FeSi phase [10]. The presence of Al, Si and β-Al_5FeSi phases in the structure of the as-compacted alloy is also proved by the XRD pattern of this alloy as seen in Fig. 6. The XRD pattern is dominated by peaks assigned to the Al and β-Al_5FeSi phases. The number of peaks assigned to Si is low because a significant portion of silicon constitutes the ternary β-Al_5FeSi phase.

Despite the rapid solidification of the Al-13Si-10Fe alloy, its phase composition corresponds to the well known ternary equilibrium diagram of the Al-Si-Fe system [10] that is illustrated in Fig. 7. Non-equilibrium phases such as, for example, Al_4FeSi_2, were not found. In some recent papers, the Al_4FeSi_2 phase was identified in rapidly solidified Al-Si-Fe alloys with 20 wt.% of Si [4, 6]. It was observed that this phase transformed into the equilibrium β-Al_5FeSi phase during hot pressing at 400 ℃/1 h [6]. In this study, the compaction was performed at 300 ℃/5 min, so solid state phase transformations of intermetallic phases were unlikely. Therefore, the β-Al_5FeSi phase forms during the rapid solidification and the absence of the non-equilibrium Al_4FeSi_2 phase is likely caused by the lower silicon concentration in the studied alloy (Fig. 7).

The structure of the casting Al-12Si-1Cu-1Mg-1Ni

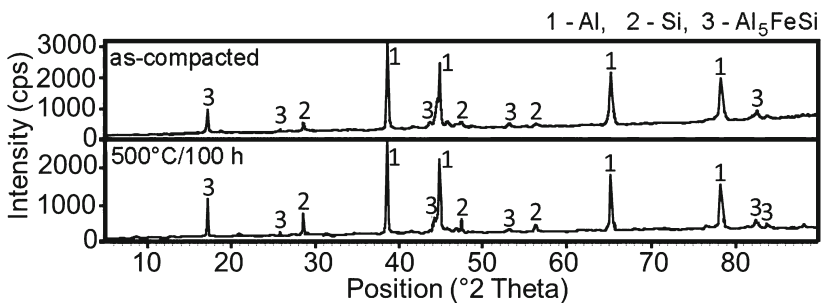

Fig. 6. XRD patterns of the Al-13Si-10Fe alloy: as-compacted, annealed at 500 ℃/100 h.

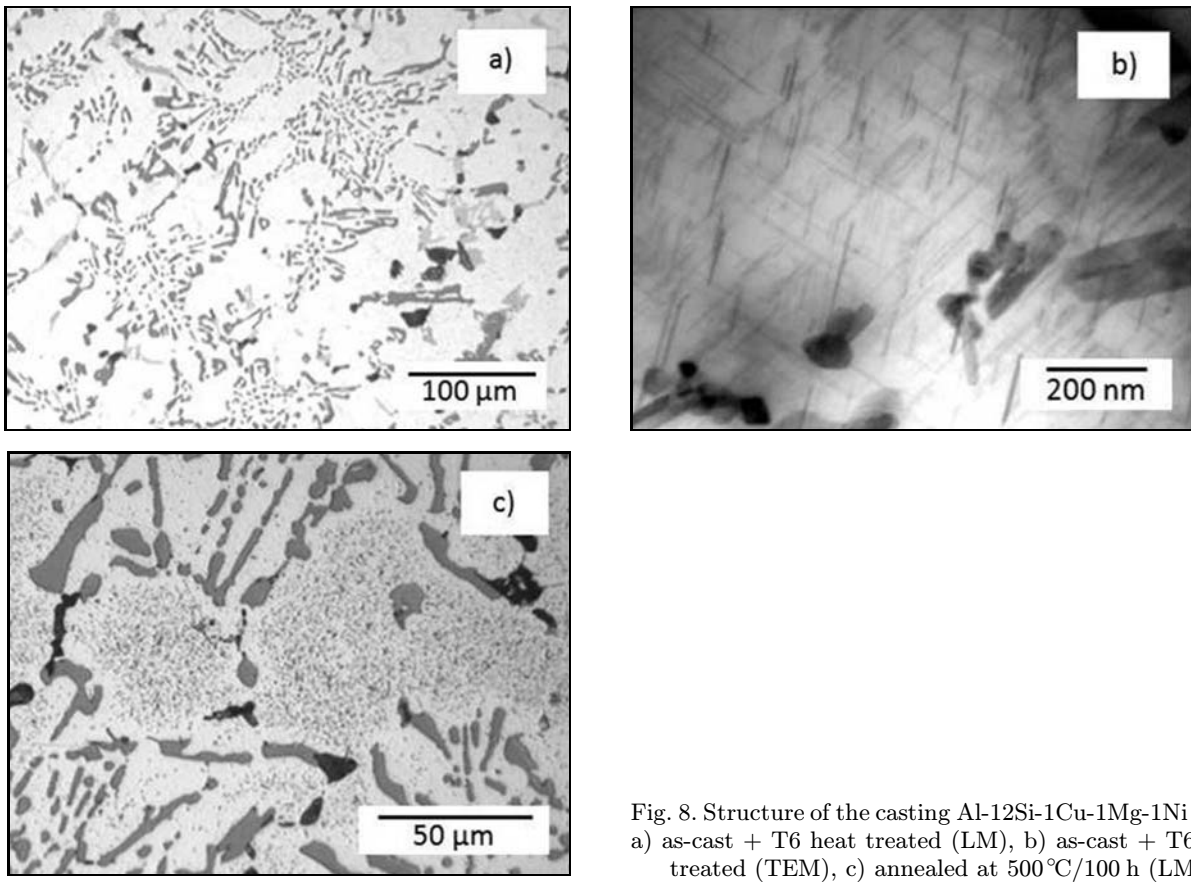

Fig. 8. Structure of the casting Al-12Si-1Cu-1Mg-1Ni alloy: a) as-cast + T6 heat treated (LM), b) as-cast + T6 heat treated (TEM), c) annealed at 500 °C/100 h (LM).

(T6) alloy is shown in Fig. 8. Figure 8a demonstrates that the structure is relatively coarse and consists of primary α(Al) dendrites (light), α(Al) + Si eutectic and intermetallic phases containing mainly Ni and Al. The average distance between dendritic branches and the diameter of the Si particles are 45 µm and 7 µm, respectively. Due to a much lower cooling rate during gravity casting, these structural parameters are seen to be significantly higher than the structural parameters of the as-compacted Al-13Si-10Fe alloy (Fig. 4). During the T6 heat treatment, plate-like $Al_2CuMgNi$ precipitates were formed which caused the final hardening of the alloy (Fig. 8b).

The influence of the 100-hour-annealing at 500 °C on the structure of the Al-13Si-10Fe alloy is shown in Figs. 4c and 6. In this alloy, two processes predominate during annealing: 1. coarsening of the eutectic silicon particles, and 2. fragmentation of the β-Al_5FeSi needle-like particles. The silicon particles grow fast from the original sub-micrometer size to several micrometers. The rapid coarsening of the Si particles is explained by both the tendency to reduce the α(Al)/Si interface area and a relatively high diffusion coefficient of silicon in solid Al (Fig. 1). Iron is characterized by a lower diffusion coefficient than silicon, and therefore, the coarsening and thickening of β-Al_5FeSi particles during annealing is slower and is not observed after 100-hour-annealing. Instead, a surprising phenomenon that is observed is the fragmentation of needle-like particles, with an original length of 30 µm, to shorter particles that have an average length of 8 µm. The thickness of the fragmented particles remains nearly the same as that of the original needles, i.e., approximately 2 µm. Both the coarsening of Si and the fragmentation of β-Al_5FeSi have a direct influence on mechanical properties, as shown in the following paragraphs. Figure 6 also indicates that annealing at 500 °C/100 h does not influence the phase composition of the Al-13Si-10Fe alloy. The annealed alloy is still dominated by the α(Al), β-Al_5FeSi and Si phases.

The detailed views in Fig. 4 suggest that the observed refining of the β-Al_5FeSi phase during annealing can be attributed to the mechanical behaviour of this phase. We observed that, as the originally long needles became fractured and formed short fragments, the spaces between these fragments are filled with the α(Al) matrix. It can be assumed that annealing at the high temperature induces internal micro-stresses in the alloy, possibly due to differences in thermal expansion and elastic moduli of the present phases, which cause the needle-like particles to crack. Once a micro-crack is created, it serves as a good diffusion path for Al atoms. As a result, the space between fragments is progressively replaced with Al. An additional driving force of this process is a reduction of free surfaces of

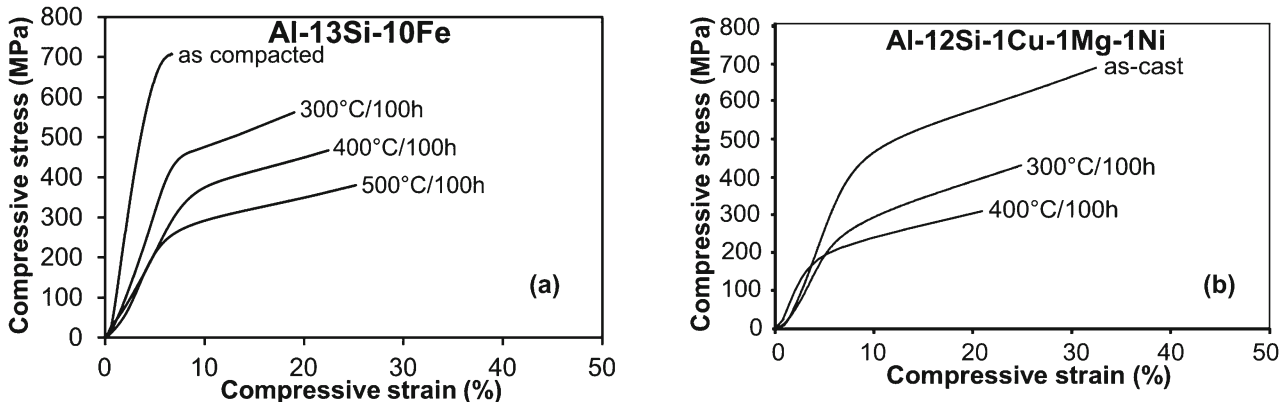

Fig. 9. Compressive stress-strain diagrams of the alloys in various states: a) PM Al-13Si-10Fe alloy, b) casting Al-12Si-1Cu-1Mg-1Ni alloy.

Table 2. Mechanical properties of the PM Al-13Si-10Fe and casting Al-12Si-1Cu-1Mg-1Ni alloys

Alloy (state)	Vickers hardness	Compressive strength (MPa)	Compressive yield strength (MPa)
Al-13Si-10Fe (as-compacted)	185	720	650
Al-13Si-10Fe (300 °C/100 h)	125	495	420
Al-13Si-10Fe (400 °C/100 h)	105	455	350
Al-13Si-10Fe (500 °C/100 h)	90	360	245
Al-12Si-1Cu-1Mg-1Ni (as-cast + T6)	130	680	430
Al-12Si-1Cu-1Mg-1Ni (300 °C/100 h)	63	420	210
Al-12Si-1Cu-1Mg-1Ni (400 °C/100 h)	65	305	175
Al-12Si-1Cu-1Mg-1Ni (500 °C/100 h)	60	–	–

both the α(Al) and β-Al_5FeSi phases.

The influence of 100-hour annealing at 500 °C on the casting Al-12Si-1Cu-1Mg-1Ni alloy is illustrated in Fig. 8c. One can observe that the eutectic silicon particles grew from the original 7 μm up to approximately 20 μm. In addition, the $Al_2CuMgNi$ precipitates, whose original size was approximately 100 nm, coarsened considerably. The precipitates now appear as dark spots inside the primary α(Al) dendrites. The reason for their growth is identical to that of the eutectic silicon, i.e., the fast diffusivities of Mg, Cu and Ni in Al (Fig. 1).

3.2. Mechanical properties and thermal stability

Figure 9 compares the compressive stress-strain diagrams of the PM Al-13Si-10Fe and the casting Al-12Si-1Cu-1Mg-1Ni alloys, both in the initial state and after annealing at 300–500 °C/100 h. Figure 10 shows the development of the room temperature Vickers hardness during annealing at 300–500 °C. The mechanical properties derived from these figures are summarized in Table 2.

It was observed that the as-compacted PM Al-13Si-10Fe alloy showed significantly higher hardness and compressive yield strength than the as-cast and T6 heat treated Al-12Si-1Cu-1Mg-1Ni alloy. This is caused by a much smaller α(Al) grain size in the PM alloy due to its rapid solidification. An additional contribution to both the hardness and yield strength is the high volume fraction of the hard phases, namely Si and β-Al_5FeSi, in the structure of the Al-13Si-10Fe alloy (Figs. 4 and 5). In contrast, the casting alloy contains large α(Al) grains, whose contribution to Hall-Petch strengthening is negligible (Fig. 8a). The most pronounced strengthening mechanism operating in this alloy is precipitation strengthening caused by semi-coherent $Al_2CuMgNi$ precipitates (Fig. 8b).

Another important finding is that the compressive strength (720 MPa) of the as-compacted Al-13Si-10Fe alloy is significantly higher than the recently reported compressive strength ($\sim$ 500 MPa) of the Al-20Si-5Fe-2(Cu, Ni, Cr) alloy [6]. However, those samples were compacted both at a higher temperature (400 °C) and for a longer time (60 min). This suggests that the ultra-high-pressure compaction at 300 °C/5 min that was used in our experiment did not induce excessive structural changes and softening.

The PM Al-13Si-10Fe alloy shows certain plasticity, despite its high iron content (Fig. 9a). This behaviour may be attributed to the preparation proced-

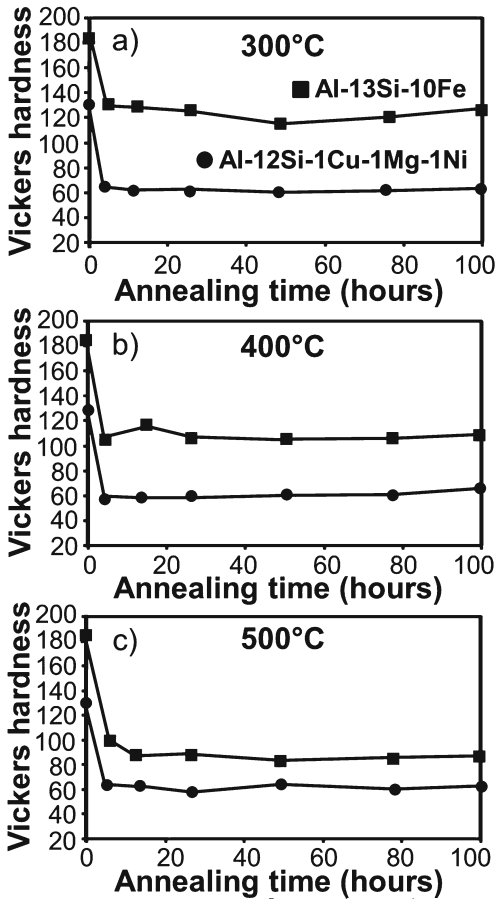

Fig. 10. Room temperature Vickers hardness as a function of annealing time at 300 °C (a), 400 °C (b) and 500 °C (c).

ure, including the rapid solidification of the melt. The needle-like β-Al_5FeSi particles (Fig. 4) are seen to always act as primary stress concentrators during compressive loading, so the Al-13Si-10Fe alloy prepared by common gravity casting would thus be extremely brittle. However, this stress concentration is proportional to longitudinal dimensions of needles, so the refining caused by rapid solidification is able to reduce the local stresses and allows the plastic α(Al) phase to be deformed before the formation of fracture micro-cracks.

Both the hardness and the compressive strength of the PM Al-13Si-10Fe alloy decrease during annealing at 300–500 °C, but these decreases occur much more slowly than in the case of the casting Al-12Si-1Cu-1Mg-1Ni alloy (Figs. 9 and 10). One explanation for the better thermal stability of the PM Al-13Si-10Fe alloy is the lower diffusivity of iron in solid aluminium as compared to silicon, copper, magnesium and nickel (Fig. 1). The coarsening of the β-Al_5FeSi particles is therefore very slow. Instead, these particles fragment during annealing which positively influences both hardness and strength (Fig. 4c). Fragmentation of the β-Al_5FeSi particles is also the reason for increasing plasticity of the PM Al-13Si-10Fe alloy after annealing (Fig. 9a). On the contrary, the casting alloy rapidly softens during annealing (Fig. 10), which can be attributed to the fast growth of precipitates in the α(Al) matrix (Fig. 8c). The measurements of the compressive strength of the Al-12Si-1Cu-1Mg-1Ni and the PM Al-13Si-10Fe alloys show higher values for the PM alloy annealed at 500 °C than for the Al-12Si-1Cu-1Mg-1Ni alloy annealed at 400 °C, therefore, the compressive strength of the latter alloy annealed at 500 °C was not measured.

4. Conclusions

It has been demonstrated in this work that the PM Al-13Si-10Fe alloy, when prepared by a combination of centrifugal atomization and high-pressure compaction, has a refined structure, which has a positive impact on strength, hardness and plasticity. The alloy also shows excellent thermal stability in comparison with the casting Al-12Si-1Cu-1Mg-1Ni alloy commonly used for the production of combustion engine pistons. The classical casting processes cannot be used for the preparation of the Al-13Si-10Fe alloy because of its high iron content, as the iron would form large needle-like β-Al_5FeSi particles, which would result in an extreme brittleness of the as-cast alloy. A positive feature of the PM process is that it involves rapid solidification of the melt that is directly related to the structural refining of the PM alloy. PM is thus shown to be a viable technology to process Al-based alloys with high-iron contents.

Acknowledgements

The authors wish to thank the Czech Science Foundation (project no. P108/12/G043) and the Czech Academy of Sciences (project no. KAN 300100801) for their financial support of this research.

References

[1] Du, Y., Chang, Y. A., Huang, B., Gong, W., Jin, Z., Xu, H., Yuan, Z., Liu, Y., He, Y., Xie, F. Y.: Mat. Sci. Eng. A-Struct., *A363*, 2003, p. 140. doi:10.1016/S0921-5093(03)00624-5

[2] Vojtech, D., Verner, J., Serak, J., Simancik, F., Balog, M., Nagy, J.: Mat. Sci. Eng. A-Struct., *A458*, 2007, p. 371.

[3] Shaw, L., Luo, H., Villegas, J., Miracle, D.: Scripta Mater., *50*, 2004, p. 921. doi:10.1016/j.scriptamat.2004.01.021

[4] Rajabi, M., Smichi, A., Vahidi, M., Davami, P.: J. Alloy. Compd., 466, 2008, p. 111. doi:10.1016/j.jallcom.2007.11.078

[5] Rajabi, M., Smichi, A., Davami, P.: Mat. Sci. Eng. A-Struct., *A492*, 2008, p. 443. doi:10.1016/j.msea.2008.03.047
[6] Rajabi, M., Vahidi, M., Smichi, A., Davami, P.: Mater. Charact., *60*, 2009, p. 1370. doi:10.1016/j.matchar.2009.06.014
[7] Srivastava, V. C., Ghosal, P., Ojha, S. N.: Mater. Lett., *56*, 2002, p. 797. doi:10.1016/S0167-577X(02)00616-X
[8] Cieslak, G., Latuch, J.: Rev. Adv. Mater. Sci., *18*, 2008, p. 425.
[9] Michna, S.: Aluminium Materials and Technologies from A to Z. Presov, Adin 2007.
[10] Mondolfo, L. F.: Aluminum Alloys: Structure and Properties. London, Butter Worths 1976.